Contribution from the Department of Chemistry, University of Houston—University Park, Houston, Texas 77004, and Laboratoire de Synthèse et d'Electrosynthèse Organométallique Associé au CNRS (LA 33), Faculté des Sciences "Gabriel", 21100 Dijon, France

Electrochemistry and Spectroelectrochemistry of Gallium(III) Porphyrins. Redox Properties of Five-Coordinate Ionic and σ-Bonded Complexes

K. M. Kadish,*[1a] B. Boisselier-Cocolios,[1a] A. Coutsolelos,[1b] P. Mitaine,[1b] and R. Guilard*[1b]

Received December 11, 1984

The electrochemistry, NMR spectroscopy, and UV–visible spectroscopy of 18 different gallium(III) porphyrins with ionic Cl^- or σ-bonded axial ligands were investigated in nonaqueous media. The ligands σ bonded to gallium(III) octaethylporphyrins or tetraphenylporphyrins included simple alkyl groups such as CH_3 or C_2H_5 and aryl groups such as C_6H_5, $C_2H_2C_6H_5$, or $C_2C_6H_5$. All of the compounds could be oxidized or reduced by multiple single-electron-transfer steps in which the initial step yields $[(P)Ga(R)]^+$ or $[(P)Ga(R)]^-$, where P represents the porphyrin macrocycle and R is one of the σ-bonded ligands. In all cases, the singly and doubly reduced compounds were stable. In contrast, the singly oxidized compounds underwent a metal–carbon bond cleavage, the rate of which depended upon the electron-donating properties of the axial ligand. The electron-donating properties of the σ-bonded ligand also influenced the electronic absorption spectra, but not the ^1H NMR spectra of the neutral compounds. The physical properties of complexes containing a bound $C_2C_6H_5$ ligand more closely resembled those of the gallium(III) porphyrin axially bound by an ionic ligand such as Cl^-. Finally, comparisons between the electrochemical reactivities of the σ-bonded complexes and their physicochemical properties are discussed in terms of the general stability of the gallium–carbon σ bond.

Introduction

Metalloporphyrins containing σ-bonded alkyl or aryl ligands have been proposed in several biological redox reactions, and because of this, a large amount of data on synthetic σ-bonded metalloporphyrin complexes has recently become available.[2-26] The chemical reactivity of this class of compounds has also attracted interest due to their potential use in the activation of small molecules. For example, it has been shown that sulfur dioxide[27] and carbon dioxide[28] can be inserted into the metal–carbon bond of indium(III)–alkyl or –aryl porphyrins and it was demonstrated that the metal–carbon bond is photoactivated by visible light.[28]

In addition to the above, σ-bonded alkyl and aryl porphyrins are good precursors in the synthesis of bi- or trimetallic metal–metal-bonded metalloporphyrins.[29,30] Especially relevant to the synthesis of novel metal–metal-bonded dimers or trimers, is the potential use of the σ-bonded alkyl or aryl complexes as starting materials in the synthesis of linear metal-chain derivatives with high or unusual conducting properties. The most important result that has emerged from comparisons between synthetic polymeric metal–metal-bonded metalloporphyrins and the so-called "organic metals" typified by TTF/TCNQ concerns the nature of the carriers. According to initial results on several oxidized linear polymeric metalloporphyrins, the charge carriers exhibit both metal and ligand properties.[31]

Recently, one of our laboratories published the synthesis and characterization of gallium σ-bonded alkyl and aryl porphyrins[32] and the bridge-stacked polymeric structure of a complex containing fluorinated gallium(III) porphyrins.[33] These two types of complexes are remarkable precursors for conductors, and it is thus of importance to have knowledge concerning the electrochemical properties of these complexes. Related to this is the interest in knowing if a high oxidiation state of the gallium ion can be directly generated by electrochemical oxidation. This type of information would thus provide insight into the role of the gallium ion in the conduction process of the linear-chain polymer. In order to answer these questions, we have initiated a detailed electrochemical study on the oxidation and reduction of a large series of gallium(III) porphyrins that are σ bonded by both alkyl and aryl groups. The results of these studies are given in this paper. We have also

(1) (a) University of Houston. (b) University of Dijon.
(2) Reed, C. A.; Mashiko, T.; Bentley, S. P.; Kastner, M. E.; Scheidt, W. R.; Spartalian, K.; Lang, G. *J. Am. Chem. Soc.* **1979**, *101*, 2948.
(3) Lexa, D.; Saveant, J. M.; Battioni, J. P.; Lange, M.; Mansuy, D. *Angew. Chem., Int. Ed. Engl.* **1980**, *20*, 578.
(4) Ortiz de Montellano, P. R.; Kunze, K. L.; Augusto, O. *J. Am. Chem. Soc.* **1982**, *104*, 3545.
(5) (a) Cocolios, P.; Laviron, E.; Guilard, R. *J. Organomet. Chem.* **1982**, *228*, C39. (b) Cocolios, P.; Lagrange, G.; Guilard, R. *J. Organomet. Chem.* **1983**, *253*, 65.
(6) Ogoshi, H.; Sugimoto, H.; Yoshida, Z.; Kobayashi, H.; Sakai, H.; Maeda, Y. *J. Organomet. Chem.* **1982**, *234*, 185.
(7) Mansuy, D.; Battioni, J. P. *J. Chem. Soc., Chem. Commun.* **1982**, 638.
(8) Mansuy, D.; Fontecave, M.; Battioni, J. P. *J. Chem. Soc., Chem. Commun.* **1982**, 317.
(9) Mansuy, D.; Battioni, J. P.; Dupre, D.; Sartori, E.; Chottard, G. *J. Am. Chem. Soc.* **1982**, *104*, 6159.
(10) Kunze, K. L.; Ortiz de Montellano, P. R. *J. Am. Chem. Soc.* **1983**, *105*, 1380.
(11) Battioni, P.; Mahy, J. P.; Gillet, G.; Mansuy, D. *J. Am. Chem. Soc.* **1983**, *105*, 1399.
(12) Perree-Fauvet, M.; Gaudemer, A.; Boucly, P.; Devynck, J. *J. Organomet. Chem.* **1976**, *120*, 439.
(13) Callot, H. J.; Schaeffer, E. *J. Organomet. Chem.* **1978**, *145*, 91.
(14) Callot, H. J.; Schaeffer, E. *J. Organomet. Chem.* **1980**, *193*, 111.
(15) Dolphin, D.; Halko, J.; Johnson, E. *Inorg. Chem.* **1981**, *20*, 4348.
(16) Callot, H. J.; Metz, F. *J. Chem. Soc., Chem. Commun.* **1982**, *947*.
(17) Ogoshi, H.; Setsune, J.; Nanbo, Y.; Yoshida, Z. *J. Organomet. Chem.* **1978**, *159*, 329.
(18) Callot, H. J.; Schaeffer, E. *Nouv. J. Chim.* **1980**, *4*, 311.
(19) Ogoshi, H.; Setsune, J.; Yoshida, Z. *J. Organomet. Chem.* **1980**, *185*, 95.
(20) Wayland, B. B.; Woods, B. A. *J. Chem. Soc., Chem. Commun.* **1981**, *700*.
(21) Setsune, J.; Yoshida, Z.; Ogoshi, Z. *J. Chem. Soc., Perkin Trans. 1* **1982**, 983.
(22) Ogoshi, H.; Setsune, J.; Yoshida, Z. *J. Organomet. Chem.* **1978**, *159*, 317.
(23) Cloutour, C.; Lafargue, D.; Richards, J. A.; Pommier, J. C. *J. Organomet. Chem.* **1977**, *137*, 157.
(24) (a) Guilard, R.; Cocolios, P.; Fournari, P. *J. Organomet. Chem.* **1977**, *129*, C11. (b) Cocolios, P.; Guilard, R.; Fournari, P. *J. Organomet. Chem.* **1979**, *179*, 311.
(25) (a) Inoue, S.; Takeda, N. *Bull. Chem. Soc. Jpn.* **1977**, *50*, 984. (b) Takeda, N.; Inoue, S. *Bull.* Chem. *Soc. Jpn.* **1978**, *51*, 3564.
(26) Inoue, S.; Murayama, N.; Takeda, N.; Ohkatsu, Y. *Chem. Lett.* **1982**, 317.
(27) Cocolios, P.; Fournari, P.; Guilard, R.; Lecomte, C.; Protas, J.; Boubel, J. C. *J. Chem. Soc., Dalton Trans.* **1980**, 2081.
(28) Cocolios, P.; Guilard, R.; Bayeul, D.; Lecomte, C. *Inorg. Chem.* **1985**, *24*, 2058.
(29) Cocolios, P.; Moise, C.; Guilard, R. *J. Organomet. Chem.* **1982**, *228*, C43.
(30) Cocolios, P.; Chang, D.; Vittori, O.; Guilard, R.; Moise, C.; Kadish, K. M. *J. Am. Chem. Soc.* **1984**, *106*, 5724.
(31) See, for example: (a) Ibers, J. A.; Pace, L. J.; Martinsen, J.; Hoffman, B. M. *Struct. Bonding (Berlin)* **1983**, *50*, 1. (b) Hoffman, B. M.; Ibers, J. A. *Acc. Chem. Res.* **1983**, *16*, 15.
(32) Coutsolelos, A.; Guilard, R. *J. Organomet. Chem.* **1983**, *253*, 273.
(33) Goulon, J.; Friant, P.; Goulon-Ginet, C.; Coutsolelos, A.; Guilard, R. *Chem. Phys.* **1984**, *83*, 367.

0020-1669/85/1324-4521$01.50/0

Table I. Maximum Absorbance Wavelengths (λ_{max}) and Corresponding Molar Absorptivities ($\epsilon \times 10^{-3}$) for Neutral (TPP)GaCl and (TPP)Ga(R) Complexes in C_6H_6[a]

axial ligand, R	band I	B(1,0)	band II or B(0,0)	ϵ(II)/ϵ(I)	Q(2,0)	Q(1,0)	Q(0,0)
Cl		397 (18.0)	418 (524.4)		548 (20.7)	587 (4.5)	621 (1.3)
$C(CH_3)_3$	379 (6.5)		446 (13.3)	2.04	551 (0.3)	579 (0.9)	626 (0.8)
C_4H_9	347 (3.9)		441 (23.0)	6.22	531 (0.5)	573 (1.2)	617 (1.0)
C_2H_5	346 (31.7)		441 (211.0)	6.66	535 (3.3)	573 (9.6)	618 (8.3)
CH_3	337 (35.7)		436 (326.9)	9.16	531 (4.4)	570 (4.9)	612 (7.3)
C_6H_5	334 (3.8)		436 (35.5)	9.34	524 (0.5)	567 (1.5)	608 (1.0)
p-MeC_6H_4	336 (23.0)		435 (231.1)	11.43	528 (2.5)	568 (10.6)	610 (6.9)
$C_2H_2C_6H_5$	335 (10.0)		434 (128.8)	12.90	537 (0.8)	566 (4.4)	608 (2.6)
$C_2C_6H_5$	328 (27.1)		420 (549.0)	20.20	549 (2.1)	590 (7.8)	631 (3.9)

[a] Wavelengths in nm; molar absorptivities are given in parentheses following the wavelengths.

Table II. Maximum Absorbance Wavelengths (λ_{max}) and Corresponding Molar Absorptivities ($\epsilon \times 10^{-3}$) for Neutral (OEP)GaCl and (OEP)Ga(R) Complexes in C_6H_6[a]

axial ligand, R	band I	B(1,0)	band II or B(0,0)	ϵ(II)/ϵ(I)	Q(2,0)	Q(1,0)	Q(0,0)
Cl		377 (15.9)	400 (626.5)		492 (8.9)	530 (33.2)	567 (45.9)
$C(CH_3)_3$	365 (31.0)		436 (28.4)	0.91	518 (0.2)	556 (0.5)	585 (0.2)
C_4H_9	338 (36.7)		431 (81.4)	2.22	511 (1.7)	551 (9.9)	586 (4.6)
C_2H_5	358 (62.9)		432 (148.1)	2.35	515 (3.2)	552 (17.5)	587 (8.3)
CH_3	349 (41.7)		426 (185.7)	4.45	509 (2.9)	549 (15.3)	586 (9.4)
C_6H_5	348 (13.4)		423 (64.2)	4.79	507 (1.4)	547 (4.9)	587 (3.6)
p-MeC_6H_4	350 (8.5)		424 (43.3)	5.09	505 (0.6)	546 (3.2)	582 (2.1)
$C_2H_2C_6H_5$	333 (11.8)		403 (131.4)	11.13	490 (1.4)	533 (5.6)	572 (7.9)
$C_2C_6H_5$	334 (25.3)		402 (399.3)	15.18	492 (2.9)	532 (16.3)	572 (24.6)

[a] Wavelengths in nm; molar absorptivities are given in parentheses following the wavelengths.

included in this paper the related electrochemistry of the chlorogallium(III) porphyrins. These complexes are the precursors in the synthesis of the σ-bonded complexes.

Experimental Section

Electrochemical Instrumentation. Cyclic voltammetric measurements were carried out with either an EG&G Model 173 potentiostat and EG&G Model 175 universal programmer, or a BAS 100 electrochemical analyzer. Current–voltage curves were recorded on a Houston Instrument Model 2000 X-Y recorder, a Houston Instrument HIPLOT DMP-40 plotter, or an EPSON Model FX 80 printer. A three-electrode system was used with a Pt-button working electrode and a Pt-wire counter electrode. A saturated calomel electrode (SCE) was used as the reference and was separated from the bulk of the solution by a fritted glass bridge. Controlled-potential electrolysis was performed in a bulk cell where the SCE reference electrode and the Pt-wire counter electrode were separated from the test solution by fritted glass bridges containing solvent and supporting electrolyte. A BAS 100 electrochemical analyzer was used to control the potential.

Spectroscopic Instrumentation. Spectroelectrochemical experiments were performed with an IBM Model EC 225 voltammetric analyzer coupled with a Tracor Northern 1710 holographic optical spectrometer/multichannel analyzer to obtain time-resolved spectral data. The Pt thin-layer cell used has been described elsewhere.[34] UV–visible spectra were also taken by using a Perkin-Elmer 559 spectrophotometer. ESR spectra were recorded either with a Varian E4 X-band spectrometer or an IBM Model ER 100 D spectrometer equipped with a Model ER 040-X microwave bridge and a Model ER 080 power supply. Infrared spectra were taken on a Perkin-Elmer 580 B apparatus. Samples were prepared as 1% dispersions in CsI pellets or as Nujol mulls. ^1H NMR spectra were recorded on a JEOL FX 100 spectrometer. Spectra were measured on 0.5-mL $CDCl_3$ or C_6D_6 solutions using tetramethylsilane as internal reference.

Chemicals. Reagent grade methylene chloride (CH_2Cl_2) and benzonitrile (PhCN) were distilled over P_2O_5 before use. Tetrabutylammonium hexafluorophosphate (TBA(PF_6)) (Fluka) was recrystallized from ethyl acetate. (TPP)GaCl and (OEP)GaCl were synthesized according to literature procedures.[32] (TPP)Ga(R) and (OEP)Ga(R), where R stands for C_4H_9, C_2H_5, CH_3, C_6H_5, and p-MeC_6H_4, were prepared according to a previously reported method[32] and characterized by IR and UV–visible spectroscopic methods. The new compounds, (TPP)Ga($C(CH_3)_3$), (TPP)Ga($C_2H_2C_6H_5$), (TPP)Ga($C_2C_6H_5$), (OEP)Ga($C(CH_3)_3$), (OEP)Ga($C_2H_2C_6H_5$), and (OEP)Ga($C_2C_6H_5$) were obtained by following the method described in ref 32. The synthesis and handling of these complexes were carried out under an atmosphere of argon. All common solvents were thoroughly dried in an appropriate manner and were distilled under argon prior to use. All operations were carried out in Schlenk tubes under purified argon and with dried oxygen-free solvents. Their UV–visible data are given in Tables I and II, and the characteristic IR vibrations and NMR data of the (TPP)Ga(R) and (OEP)Ga(R) complexes are given in Tables III and IV.

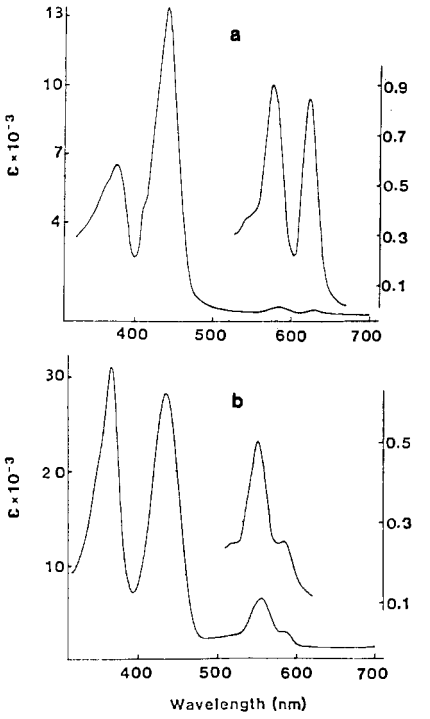

Figure 1. Electronic absorption spectrum of (a) (TPP)Ga($C(CH_3)_3$) and (b) (OEP)Ga($C(CH_3)_3$) in C_6H_6.

Results and Discussion

Spectroscopic Properties of Ionic (P)GaCl and Neutral (P)Ga(R). The electronic absorption spectra of (TPP)GaCl and (OEP)GaCl are classified as "normal" porphyrin spectra.[35] For example, (TPP)GaCl has a Soret band at 418 nm and in the same region a B(1,0) blue-shifted band at 397 nm. In addition, three

(34) Lin, X.; Kadish, K. M. *Anal. Chem.* **1985**, *57*, 1498.

(35) Gouterman, M. In "The Porphyrins"; Dolphin, D., Ed.; Academic Press: New York, 1978; Vol. III, Chapter 1 and references therein.

Table III. ^{1}H NMR and IR Data for the (TPP)Ga(R) and (TPP)Ga(Cl) Complexes[b]

		methine protons		phenylic protons		protons of R (Ar)		
complexes	R (Ar)	m/i[c]	δ	m/i[c]	δ	m/i[c]	δ	ν_{Ga-R}, cm^{-1}
(TPP)GaCl[a]		s/8	9.07	m/8 (*o*-H)	8.20			352 (ν_{Ga-Cl})
				m/12 (*m*,*p*-H)	7.76			
(TPP)Ga(CH_3)[a]	CH_3	s/8	8.97	m/8 (*o*-H)	8.18	s/3	−6.22	557
				m/12 (*m*,*p*-H)	7.73			
(TPP)Ga(CH_2CH_3)[a]	CH_2CH_3	s/8	8.98	m/8 (*o*-H)	8.20	t/3	−3.34	542
				m/12 (*m*,*p*-H)	7.74	q/2	−5.66	
(TPP)Ga($(CH_2)_3CH_3$)[a]	$(CH_2)_3CH_3$	s/8	8.98	m/8 (*o*-H)	8.18	m/2 (α-CH_2)	−5.64	468
				m/12 (*m*,*p*-H)	7.74	m/2 (β-CH_2)	−3.34	
						m/2 (γ-CH_2)	−1.50	
						t/3 (δ-CH_3)	−0.60	
(TPP)Ga(C_6H_5)[a]	C_6H_5	s/8	9.01	m/8 (*o*-H)	8.17	m/2 (*o*-H)	1.96	454
				m/12 (*m*,*p*-H)	7.75	m/2 (*m*-H)	5.41	
						m/1 (*p*-H)	5.9	
(TPP)Ga(p-$CH_3C_6H_4$)[a]	*p*-$CH_3C_6H_4$	s/8	8.99	m/8 (*o*-H)	8.15	d/2 (*o*-H)	1.90	483
				m/12 (*m*,*p*-H)	7.71	q/2 (*m*-H)	5.24	
						s/3 (*p*-CH_3)	1.29	
(TPP)Ga($C(CH_3)_3$)	$C(CH_3)_3$	s/8	9.09	m/8 (*o*-H)	8.13			
				m/12 (*m*,p-H)	7.74	s/9 (−$C(CH_3)_3$)	−3.10	468
(TPP)Ga($C_2H_2C_6H_5$)	CH=CHC_6H_5	s/8	9.12	m/8 (*o*-H)	8.09	m/2 (*o*-H)	5.51	
				m/12 (*m*,*p*-H)	7.42	m/3 (*m*,*p*-H)	6.28	730
						d/1 (−CH=*CH*−)	1.86	
						d/1 (−*CH*=CH−)	1.72	
(TPP)Ga($C_2C_6H_5$)	C≡CC_6H_5	s/8	9.01	m/8 (*o*-H)	8.20	m/2 (*o*-H)	5.9	567
				m/12 (*m*,*p*-H)	7.77	m/3 (*m*,*p*-H)	6.6	

[a] From ref 32. [b] In C_6D_6, Me_4Si reference. [c] Key: *m* = number of lines; *i* = number of protons; s = singlet; d = doublet; t = triplet; q = quadruplet; m = multiplet.

Table IV. ^{1}H NMR and IR Data for the (OEP)Ga(R) and (OEP)GaCl Complexes[b]

		methylic protons		ethylic protons		protons of R (Ar)		
complexes	R (Ar)	m/i[c]	δ	m/i[c]	δ	m/i[c]	δ	ν_{Ga-C}, cm^{-1}
(OEP)GaCl[a]		s/4	10.32	t/24	1.96			332 (ν_{Ga-Cl})
				q/16	4.15			
(OEP)GaCH_3[a]	CH_3	s/4	10.17	t/24	1.93	s/3	−6.76	560
				q/16	4.14			
(OEP)Ga(CH_2CH_3)[a]	CH_2CH_3	s/4	10.17	t/24	1.92	t/3	−3.79	542
				q/16	4.15	q/2	−6.15	
(OEP)Ga($(CH_2)_3CH_3$)[a]	$(CH_2)_3CH_3$	s/4	10.16	t/24	1.92	m/2 (α-CH_2)	−6.15	470
				q/16	4.15	m/2 (β-CH_2)	−3.74	
						m/2 (γ-CH_2)	−1.79	
						t/3 (δ-CH_3)	−0.80	
(OEP)Ga(C_6H_6)[a]	C_6H_5	s/4	10.20	t/24	1.92	m/2 (*o*-H)	1.61	455
				q/16	4.14	m/2 (*m*-H)	5.17	
						m/1 (*p*-H)	5.60	
(OEP)Ga(*p*-$CH_3C_6H_4$)[a]	*p*-$CH_3C_6H_4$	s/4	10.19	t/24	1.92	q/2 (*o*-H)	1.55	482
				q/16	4.13	s/3 (*p*-CH_3)	1.50	
						d/2 (*m*-H)	5.01	
(OEP)Ga($C(CH_3)_3$)	$C(CH_3)_3$	s/4	10.34	t/24	1.92	s/9 (−$C(CH_3)_3$)	−3.43	470
				q/16	4.04			
(OEP)Ga($C_2H_2C_6H_5$)	CH=CHC_6H_5	s/4	10.37	t/24	1.94	m/2 (*o*-H)	5.65	730
				q/16	4.14	m/3 (*p*,*m*-H)	6.48	
						d/1 (−CH=*CH*)	1.66	
						d/1 (−*CH*=CH)	1.52	
(OEP)Ga($C_2C_6H_5$)	C≡C-C_6H_5	s/4	10.39	t/24	1.94	m/2 (*o*-H)	5.76	566
				q/16	4.16	m/3 (*m*,*p*-H)	6.48	

[a] From ref 32. [b] In C_6D_6, Me_4Si reference. [c] Key: *m* = number of lines; *i* = number of protons; s = singlet; d = doublet; t = triplet; q = quadruplet; m = multiplet.

Q bands appear at 548, 587, and 621 nm. In contrast, the σ-bonded gallium porphyrins show electronic absorption spectra belonging to the hyperclass.[35] For the series of tetraphenylporphrin complexes, the Soret band is split into two bands(labeled band I and band II), which appear between 320 and 450 nm. For all of the compounds the B(1,0) band is observed close to 420 nm and the three Q bands are located at ~540, 570, and 615 nm. This is summarized in Table I. The (OEP)Ga(R) octaethylporphyrin derivatives exhibit similar spectral characteristics, as shown in Table II. Bands I and II appear in the range 330–440 nm, while the three Q bands (Q(2,0), Q(1,0), and Q(0,0)) are located close to 505, 550, and 580 nm, respectively. This is illustrated in Figure 1, which shows electronic absorption spectra of (TPP)Ga($C(CH_3)_3$) and (OEP)Ga($C(CH_3)_3$) in C_6H_6. As can be seen in Tables I and II the ratio of the molar absorptivities for the split Soret peaks varies as a function of the different R groups. Moreover, for a given axial ligand, the ratio is higher for the tetraphenyporphyrin complexes than for the octaethylporphyrin derivatives.

The spectroscopic properties of σ-indium–carbon porphyrins[36] are similar to properties of the σ-gallium–carbon complexes. For complexes in the indium series, the presence of a blue-shifted band I was attributed to a $5p_z \rightarrow e_g(\pi^*)$ transition while band II may

(36) Kadish, K. M.; Boisselier-Cocolios, B.; Cocolios, P.; Guilard, R. *Inorg. Chem.* **1985**, *24*, 2139.

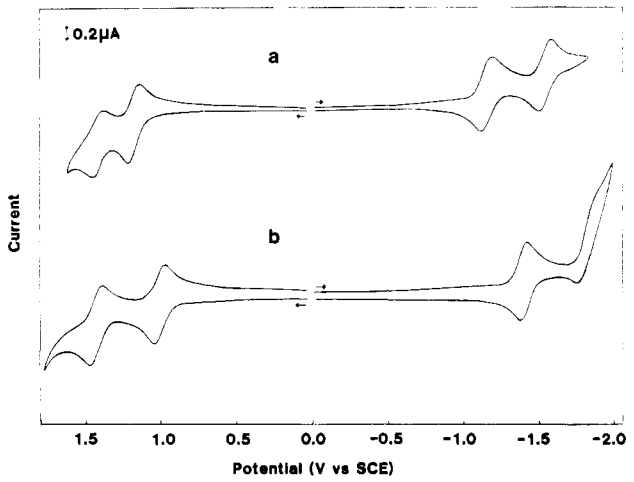

Figure 2. Cyclic voltammograms of (a) (TPP)GaCl and (b) (OEP)GaCl in CH_2Cl_2, 0.1 M $TBA(PF_6)$ (scan rate 100 mV/s).

be interpreted as a $\pi \rightarrow \pi^*$ electronic transition of the porphyrin ring. Band I of the gallium series may be attributable to $4p_z \rightarrow e_g(\pi^*)$ transition, while band II is assigned as a $\pi \rightarrow \pi^*$ electronic transition. Also, similar to the indium series, the molar absorptivity ratio of the two bands, $\epsilon(II)/\epsilon(I)$, can be related to the electron-donating ability of the axial ligand.

For a given porphyrin in one of the two series (either the tetraphenyl- or the octaethylporphyrin series), the complexes with greater electron-donating R groups have a smaller $\epsilon(II)/\epsilon(I)$ ratio. This is seen in Tables I and II, where the ratio of the molar absorptivities range between 2.04 for $(TPP)Ga(C(CH_3)_3)$ and 20.20 for $(TPP)Ga(C_2H_6H_5)$ in the tetraphenylporphyrin series. The corresponding octaethylporphyrin systems have values of $\epsilon(II)/\epsilon(I)$ that range from 0.91 for $(OEP)Ga(C(CH_3)_3)$ to 15.18 for $(OEP)Ga(C_2C_6H_5)$. The hypercharacter is normally more pronounced for the OEP derivatives than for the TPP complexes. In consideration of these results, one would expect the ionic character of the metal–carbon bond to be more pronounced for the $(P)Ga(C_2C_6H_5)$ complexes since the intensity of band I is very low.

From the electronic absorption spectra, it can be deduced that the electron density in the σ-bonded gallium complexes may be considered as essentially concentrated on the gallium atom and not on the macrocyclic ring. NMR spectroscopic data are in good agreement with this conclusion. With only a few exceptions, the resonance signals of the methine protons for various octaethylmetalloporphyrins vary over a narrow range between $\delta = 10.0$ and 10.7. The exact chemical shift depends on the oxidation state of the central metal,[37] and methine resonances are observed in the following well-defined ranges: $\delta = 9.75$–10.08 for a divalent metal; $\delta = 10.13$–10.39 for a trivalent metal; $\delta = 10.30$–10.58 for a tetravalent metal; $\delta = 10.55$ for the only measured pentavalent metal; $\delta = 10.75$ for the only measured hexavalent metal. For (OEP)Ga(R), the gallium metal oxidation state is III and the observed metal proton shifts of 10.37–10.40 ppm are typical of a trivalent metal. The specific chemical shifts for each of the (OEP)Ga(R) complexes and (OEP)GaCl are given in Table IV. As seen in this table, only small and insignificant variations of the chemical shifts occur, and in contrast with the observed results for complexes of the indium series,[36] the resonances of the methinic protons do not depend on the electron-donating ability of the axial ligands. However, as will be shown in the following sections, the UV–visible data can be correlated with the electrochemical potentials for oxidation or reduction of the (P)Ga(R) complexes.

Electrode Reactions of (OEP)GaCl and (TPP)GaCl. The electrochemistry of (OEP)GaCl and (TPP)GaCl, was investigated in CH_2Cl_2 with 0.1 M $TBA(PF_6)$. Two reversible waves are observed in reduction and two waves in oxidation. This is illustrated by the voltammograms of the two compounds, represented in Figure 2. Half-wave potentials for oxidation and reduction of these complexes are given in Tables V and VI along with $E_{1/2}$ values of the σ-alkyl and σ-alkyl derivatives.

Table V. Half-Wave Potentials or Peak Potentials[a] (V vs. SCE) of (TPP)GaCl and a Series of (TPP)Ga(R) Complexes in CH_2Cl_2, 0.1 M $TBA(PF_6)$

		oxidation			reduction	
axial ligand	σ^{*b}	1st	2nd	3rd	1st	2nd
$C(CH_3)_3$	−0.30	0.76[a]	1.20	1.47	−1.31	−1.74
C_4H_9	−0.13	0.79[a]	1.19	1.47	−1.29	−1.73
C_2H_5	−0.10	0.80[a]	1.20	1.46	−1.27	−1.70
CH_3	0.00	0.86[a]	1.19	1.46	−1.29	−1.71
$C_2H_2C_6H_5$		0.99[a]	1.21	1.48	−1.24	−1.67
C_6H_5		1.05[a]	1.22	1.48	−1.22	−1.66
$C_2C_6H_5$		1.27	1.47		−1.19	−1.59
Cl		1.19	1.42		−1.16	−1.56

[a] E_{pa} measured at 100 mV/s. [b] Substituent constant for R group. See ref 47.

Table VI. Half-Wave Potentials or Peak Potentials[a] (V vs. SCE) of (OEP)GaCl and a Series of (OEP)Ga(R) Complexes in CH_2Cl_2, 0.1 M $TBA(PF_6)$

		oxidation			reduction	
axial ligand	σ^{*c}	1st	2nd	3rd	1st	2nd
$C(CH_3)_3$	−0.30	0.68[a]	1.10	1.44	−1.54	...
C_4H_9	−0.13	0.71[a]	1.10	1.45	−1.53	...
C_2H_5	−0.10	0.72[a]	1.09	1.43	−1.51	...
CH_3	0.00	0.76[a]	1.10	1.45	−1.53	...
$C_2H_2C_6H_5$		0.98[a]	1.10	1.45	−1.47	...
C_6H_5		0.89[b]	1.34[b]		−1.49	...
$C_2C_6H_5$		0.93	1.53		−1.43	...
Cl		1.01	1.45		−1.41	−1.85

[a] E_{pa} measured at 100 mV/s. [b] Half-wave potential values measured at −10 °C. [c] Substituent constant for R group. See ref 47.

The absolute potential difference between the first two reduction potentials of (TPP)GaCl is 400 mV while for (OEP)GaCl the potential difference is 440 mV. These separations between the reduction potentials are in good agreement with the 0.42 ± 0.05 V generally observed for ring-centered reductions of different metalloporphyrin complexes.[38] In contrast, the absolute potential separations between the two reversible oxidation waves are 230 and 440 mV for (TPP)GaCl and (OEP)GaCl, respectively. The reported range for successive ring-centered oxidations of metalloporphyrins is 0.29 ± 0.05 V.[38] This might suggest that the observed oxidations for (OEP)GaCl do not involve abstractions from the π ring system. However, there are other reasons for deviations to occur (such as changes in ligand binding), and more information is needed to ascertain the actual site of the electron abstractions.

Time-resolved thin-layer spectra recorded during the first one-electron reduction of (TPP)GaCl and (OEP)GaCl are represented in Figure 3, and wavelengths of maximum absorbance for the electrogenerated species are summarized in Table VII. For both complexes, 1.0 electron is added to the starting species to give a product generally characteristic of an anion radical. For both compounds, the oxidation and reduction waves are reversible on the thin-layer spectroelectrochemical time scale.

(TPP)GaCl exhibits a Soret band at 420 nm in PhCN and three Q bands at 510, 552, and 589 nm. Upon the addition of one electron, the Soret peak is shifted toward higher wavelengths (450 nm) and two broad absorptions appear at 713 and 869 nm. A similar change in the spectrum is observed after reduction of (OEP)GaCl. The neutral complex shows an intense Soret peak at 407 nm and two peaks at 535 and 573 nm. After the addition of one electron, the Soret peak decreases in intensity and shifts to 428 nm. At the same time, the two bands in the visible region

(37) Scheer, H.; Katz, J. J. In "Porphyrins and Metalloporphyrins", Smith, K. M., Ed.; Elsevier: Amsterdam, 1975; Chapter 10.

(38) Fuhrhop, J.-H.; Kadish, K. M.; Davis, D. G. *J. Am. Chem. Soc.* **1973**, *95*, 5140.

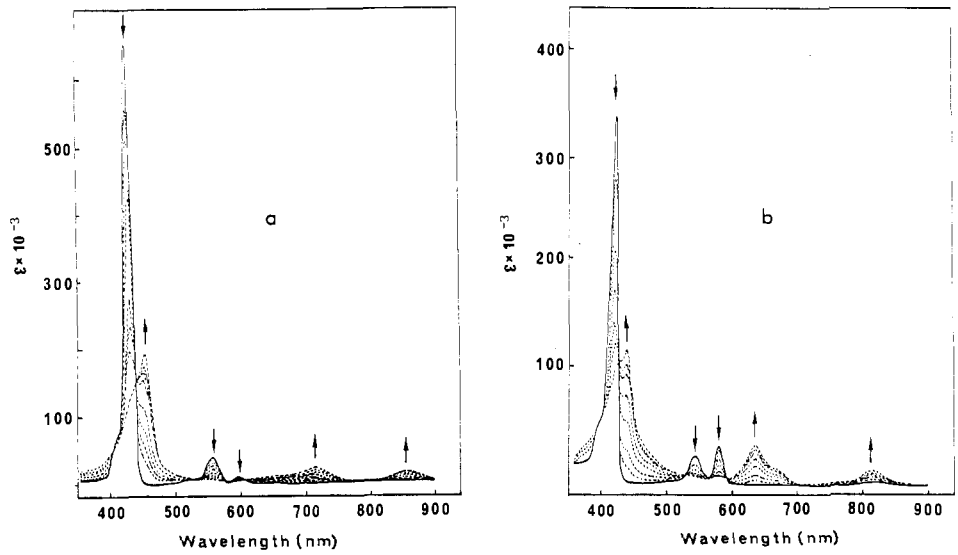

Figure 3. Time-resolved electronic absorption spectra of (a) (TPP)GaCl and (b) (OEP)GaCl recorded during a one-electron reduction in PhCN, 0.1 M $TBA(PF_6)$.

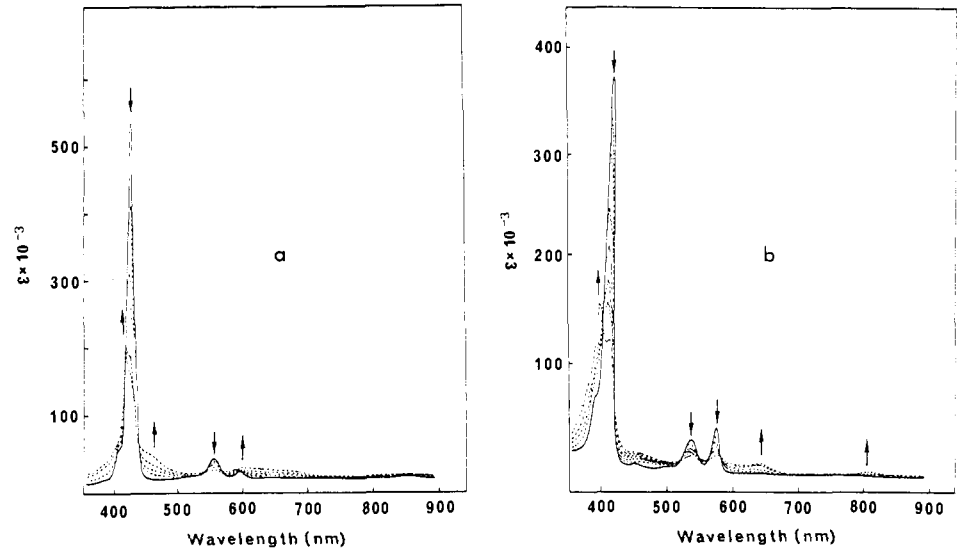

Figure 4. Time-resolved electronic absorption spectra of (a) (TPP)GaCl and (b) (OEP)GaCl recorded during a one-electron oxidation in PhCN, 0.1 M $TBA(PF_6)$.

Table VII. Maximum Absorbance Wavelengths (λ_{max}) and Corresponding Molar Absorptivities (ϵ) of Neutral, Oxidized, and Reduced (TPP)GaCl and (OEP)GaCl in PhCN, 0.1 $TBA(PF_6)$

compd	electrode reacn	λ_{max}, nm ($\epsilon \times 10^{-3}$)					
(TPP)GaCl	none	400 (5.3)	420 (634.8)	510 (4)	552 (22.6)	589 (6.0)	
	1e redn		450 (231)		713 (28)	869 (19)	
	1e oxidn		416 (211)		458 (40)	607 (10)	664 (14)
(OEP)GaCl	none	386 (54.0)	407 (370.1)		535 (17.0)	573 (24.1)	
	1e redn		428 (230)		628 (63)	659 (sh)	807 (23)
	1e oxidn		395 (291)		645 (18)		

disappear while three broad peaks that are characteristic of an anion radical appear at 628, 659, and 807 nm. These spectral changes are totally reversible, and the spectrum of the starting species can be regenerated upon application of a controlled potential more positive than −0.9 V for (TPP)GaCl and more positive than −1.2 V for (OEP)GaCl.

An assignment of the site of the first electron abstraction of the chloro complexes (π ring or metal center) is less clear-cut. This is illustrated by the electronic absorption spectra of the singly oxidized (OEP)GaCl and (TPP)GaCl derivatives, represented in Figure 4. Both compounds exhibit a shift of the Soret peak maximum toward lower wavelengths as well as a decrease in the intensity of the peak upon oxidation. In addition, the peaks in the visible region disappear but no broad absorptions are detected above 700 nm. At the same time, $[(TPP)GaCl]^+$ shows a new absorption at 457 nm and $[(OEP)GaCl]^+$ at 641 nm.

ESR of Oxidized and Reduced (TPP)GaCl and (OEP)GaCl. The complete electrolysis of (TPP)GaCl at −1.3 V in CH_2Cl_2 with 0.1 M $TBA(PF_6)$ leads to a solution whose ESR spectrum is shown in Figure 5. The g factor is close to the free-spin value of 2.0032, and the total width of about 50 G is typical of metalloporphyrin radical anions.[39,40] This observation is in accordance with the results of spectroelectrochemistry that suggest a ring-centered reduction.

(39) Felton, R. H.; Linschitz, H. *J. Am. Chem. Soc.* **1966**, *88*, 1113.
(40) Fajer, J.; Davis, M. S. In "The Porphyrins"; Dolphin, D., Ed.; Academic Press: New York, 1978; Vol. IV, Chapter 4 and references therein.

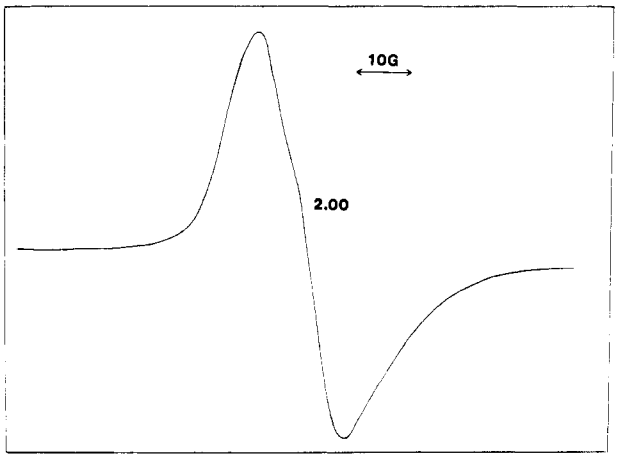

Figure 5. ESR spectrum of singly reduced (TPP)GaCl at 115 K in CH_2Cl_2, 0.1 M TBA(PF_6).

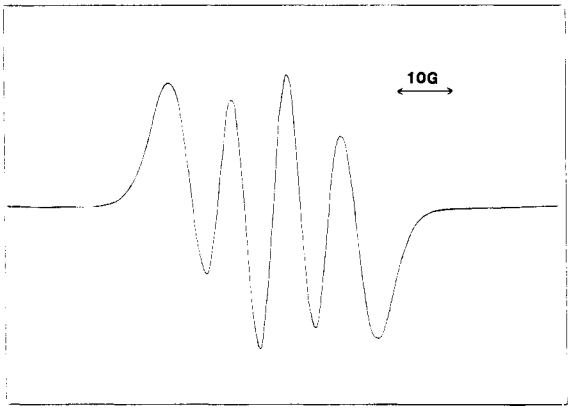

Figure 6. Room-temperature ESR spectrum of singly oxidized (TPP)GaCl in CH_2Cl_2, 0.1 M TBA(PF_6).

The one-electron oxidation of (TPP)GaCl at +1.3 V leads to a species that exhibits an ESR spectrum at room temperature. This spectrum is shown in Figure 6 and consists of four well-resolved lines reflecting coupling of the unpaired electron with the nuclear spin of gallium (A = 10 G). The natural abundances of ^{69}Ga and ^{71}Ga are 60.2 and 39.8%, respectively, and the nuclear spin is $^3/_2$ for both isotopes. At room temperature, specific lines attributable to each isotope cannot be distinguished since only four broad lines appear. The morphology of the spectrum does not show significant differences at lower temperatures and corresponds to highly isotropic ESR signals.

Delocalization of spin onto the metal of the porphyrin has been detected for oxidized cobalt,[40,41] zinc,[42-44] thallium,[45] and indium[36] complexes. With the exception of thallium porphyrins, the ESR and UV–visible spectra of these derivatives are typified by those of oxidized zinc tetraphenylporphyrin, $[(TPP)Zn]^{+\cdot}$. This latter compound exhibits an optical spectrum characteristic of an A_{2u} state, and enough spin density is found on the metal to yield detectable coupling constants. However, all of the above complexes have a small amount of spin density on the metal ion. In contrast, the octaethylporphyrin radicals $[(OEP)Mg]^{+\cdot}$, $[(OEP)Zn]^{+\cdot}$, and $[(OEP)InCl]^{+\cdot}$ have optical spectra typical of an A_{1u} state and display no metal interactions.[40] The one-electron oxidation of (OEP)GaCl also gives a radical with a singlet ESR signal that

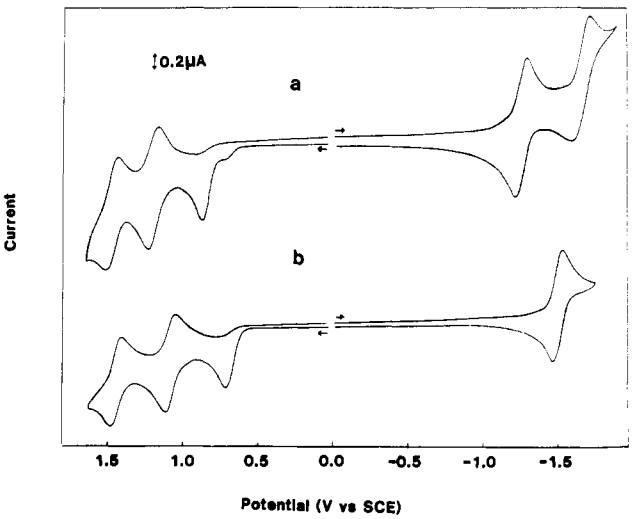

Figure 7. Cyclic voltammograms of (a) (TPP)Ga(CH_3) and (b) (OEP)Ga(CH_3) in CH_2Cl_2, 0.1 M TBA(PF_6). Scan rate 100 mV/s.

is independent of temperature. The g factor and line width of this signal are comparable to those obtained for porphyrin π cations in an A_{1u} state.

The origin of the metal interaction for $[(TPP)GaCl]^{+\cdot}$ is identical with that proposed for the cobalt, zinc, and indium series and arises from a σ–π spin-polarization mechanism. However, if a gallium interaction is clearly demonstrated, the observed splittings account for a spin density of only about 0.003% at the gallium nucleus. This calculation is made considering that the optimal hyperfine coupling constants of ^{69}Ga and ^{71}Ga are 2657.7 and 3377.0 G, respectively.[46] Consequently, the coupling constant of the unpaired electron with the nuclear spin of the gallium may be interpreted as a superhyperfine coupling, with the electron being located on the macrocycle ring.

Reductions of (TPP)Ga(R) and (OEP)Ga(R). Half-wave potentials for oxidation and reduction of (TPP)Ga(R) and (OEP)Ga(R), where R = CH_3, C_2H_5, C_4H_9, $C(CH_3)_3$, $C_2H_2C_6H_5$, C_6H_5, and $C_2C_6H_5$, are summarized in Tables V and VI, and cyclic voltammograms of (TPP)Ga(CH_3) and (OEP)Ga(CH_3) are represented in Figure 7. These voltammograms are quite representative of each compound in the OEP and the TPP series.

The tetraphenylporphyrin complexes exhibit two reduction waves while the octaethylporphyrin derivatives show only one wave in the potential range of the solvent. Half-wave potentials for the first reduction of (TPP)Ga(R) range from −1.31 to −1.19 V, and the value of $E_{1/2}$ is directly related to the substituent constant associated with the bound R group.[47] This is shown in Table V. The absolute potential difference between $E_{1/2}$ of the first and the second reduction of (TPP)Ga(R) ranges from 400 to 440 mV. This is comparable to the 400-mV value observed for reduction of (TPP)GaCl and is characteristic of ring-centered reactions. For the (OEP)Ga(R) series, the values of $E_{1/2}$ range from −1.54 V for (OEP)Ga($C(CH_3)_3$) to −1.43 V for (OEP)Ga($C_2H_6H_5$). The half-wave potentials for this series of compounds also parallel the magnitude of the substituent constant of the bound R group. However, the overall substituent effect is very small since, in both series, the shift is only 110 mV between the most difficult to reduce and the most easily reduced compound. This indicates that there is only a slight interaction of the substituent group with the electroreduction site.

Thin-layer spectroelectrochemistry was carried out for both series of compounds in PhCN with 0.1 M TBA(PF_6). Half-wave potentials recorded in that medium were quite similar to those observed in CH_2Cl_2 and varied by less than 5 mV from values obtained by normal cyclic voltammetry. The thin-layer voltam-

(41) Wolberg, A.; Manassen, J. *J. Am. Chem. Soc.* **1966**, *88*, 1113.
(42) Fajer, J.; Borg, D. C.; Forman, A.; Dolphin, D.; Felton, R. M. *J. Am. Chem. Soc.* **1970**, *92*, 3451.
(43) Fajer, J.; Borg, D. C.; Forman, A.; Adler, A. D.; Varadi, V. *J. Am. Chem. Soc.* **1974**, *96*, 1238.
(44) Fajer, J.; Borg, D. C.; Forman, A.; Felton, R. H.; Vehg, C.; Dolphin, D. *N.Y. Acad. Sci.* **1973**, *206*, 349.
(45) Mengersen, C.; Subramanian, J.; Fuhrhop, J. M.; Smith, K. M. *Z. Naturforsch., B: Anorg. Chem., Org. Chem.* **1974**, 1827.
(46) Froese, C. *J. Chem. Phys.* **1966**, *45*, 1417.
(47) Values of σ^* were taken from: Taft, R. W., Jr. In "Steric Effects in Organic Chemistry"; Newman, M. S., Ed.; Wiley: New York, 1956; Chapter 13.

Table VIII. Maximum Absorbance Wavelengths (λ_{max}) and Corresponding Molar Absorptivities (ϵ) of the Singly Reduced (OEP)Ga(R) and (TPP)Ga(R)

porphyrin	R group	λ_{max}, nm ($\epsilon \times 10^{-3}$)				
TPP	$C(CH_3)_3$	392 (35)	461 (75)	648 (21)	704 (22)	841 (20)
	C_4H_9	355 (41)	453 (110)	651 (15)	705 (17)	840 (16)
	C_2H_5	354 (31)	452 (101)	650 (9)	710 (21)	835 (30)
	CH_3	342 (31)	447 (130)	648 (25)	691 (24)	832 (35)
	$C_2H_2C_6H_5$		435 (122)	651 (20)	688 (51)	839 (20)
	C_6H_5		441 (105)		705 (20)	825 (31)
	$C_2C_6H_5$		432 (149)	647 (23)	841 (20)	
OEP	$C(CH_3)_3$	388 (51)	479 (90)		759 (35)	878 (37)
	C_4H_9	356 (81)	471 (220)		767 (34)	869 (30)
	C_4H_9	372 (62)	476 (105)		768 (41)	869 (31)
	C_2H_5	357 (66)	472 (120)		772 (50)	859 (54)
	CH_3	352 (88)	459 (208)		796 (29)	857 (41)
	$C_2H_2C_6H_5$	368 (82)	448 (201)		766 (31)	871 (35)
	C_6H_5	359 (42)	453 (221)		747 (43)	875 (33)

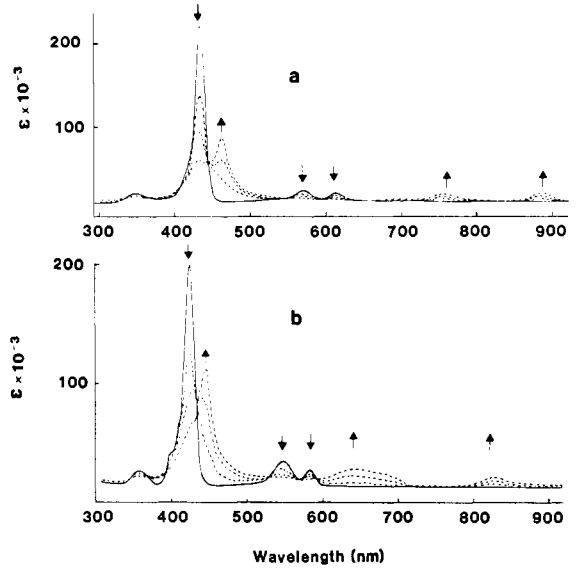

Figure 8. Time-resolved electronic absorption spectra of (a) (TPP)Ga(CH_3) and (b) (OEP)Ga(CH_3) during a one-electron reduction in PhCN, 0.1 TBA(PF_6).

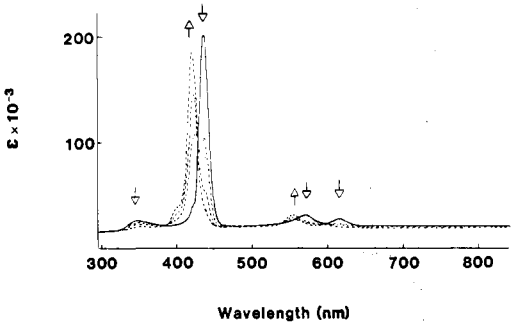

Figure 9. Time-resolved electronic absorption spectra of (TPP)Ga(CH_3) during a one-electron oxidation in PhCN, 0.1 M TBA(PF_6).

mograms were reversible, and the spectra of the starting species could be regenerated by back-electrolysis at potentials more positive than −1.0 V.

Time-resolved electronic absorption spectra of singly reduced (TPP)Ga(CH_3) and (OEP)Ga(CH_3) are represented in Figure 8 and are quite representative of the respective (TPP)Ga(R) and (OEP)Ga(R) series. Wavelengths for maximum absorbances of the singly reduced (P)Ga(R) are summarized in Table VIII. As seen in Figure 8 and Table VIII, the one-electron reduction of each σ-bonded gallium derivative leads to the formation of a species that exhibits an anion radical-like spectra. The spectrum morphologies resemble, but are not identical with, the corresponding singly reduced (P)GaCl (see Table VII).

Analysis of the electronic absorption spectra leads to conclusions that are in agreement with those from analysis of the ESR spectra obtained in the same medium. After a one-electron reduction, (TPP)Ga(CH_3) exhibits a sharp ESR signal centered at $g = 2.00$. The width of the signal is 60 G, and the symmetry of the peak is characteristic of porphyrin anion radicals. It thus appears to be conclusive that the one-electron reduction of (P)Ga(R) complexes leads to a ring-centered reduction with no interaction between the added electron and the metal center.

Oxidations of (TPP)Ga(R) and (OEP)Ga(R). Cyclic voltammograms of (P)Ga(R), where R = $C(CH_3)_3$, C_4H_9, C_2H_5, CH_3, and $C_2H_2C_6H_5$; show three oxidation waves, the first of which is irreversible as illustrated in Figure 7. When R = C_6H_5, a partial reversibility is observed for the first oxidation of the OEP derivative. If the temperature is lowered to −10 °C, the ratio of anodic and cathodic peak currents becomes closer to a theoretical value of 1.0 for this compounds, and currents for the second and third oxidation waves decrease in intensity. At the same time, a new peak appears at 1.34 V. These observations are in accordance with an EC mechanism (chemical reaction following electron transfer) for the first oxidation. This conclusion is strengthened by the similarity of the half-wave potentials for the second and third oxidations of the remaining complexes in the series. For these species, the second and third oxidations are attributed to reactions of the (P)Ga(PF_6) derivatives, which are formed after a cleavage of the Ga–C bond as shown in eq 1 and 2.

$$(P)Ga(R) \overset{e^-}{\rightleftharpoons} [(P)Ga(R)]^{+\cdot} \quad (1)$$

$$[(P)Ga(R)]^{+\cdot} \xrightarrow{k_f} [(P)Ga]^+ + R\cdot \quad (2)$$

In contrast to the above series of compounds, the (OEP)Ga($C_2C_6H_5$) and (TPP)Ga($C_2C_6H_5$) voltammograms show only two reversible oxidation waves, as illustrated by the values of $E_{1/2}$ in Tables V and VI. Thus, on the cyclic voltammetry time scale, the singly oxidized (P)Ga(R) complexes exhibit a different stability as a function of the bound R group. The peak potentials also show a progressive shift which follows the magnitude of the substituent constant associated to the bound R group.[47] For the OEP series, the values of E_p for oxidation range from 0.68 V for (OEP)Ga($C(CH_3)_3$) to 0.98 V for (OEP)Ga($C_2H_2C_6H_5$). In the TPP series, the values range from 0.76 V for (TPP)Ga($C(CH_3)_3$) to 0.99 V for (TPP)Ga($C_2H_2C_6H_5$). Such a large potential shift (300 mV) is indicative of a large range of rate constants for the chemical reaction shown by eq 2.[48]

Although some of the oxidized species are stable on the cyclic voltammetry time scale, it was not possible to identify the spectra of the oxidized species by thin-layer spectroelectrochemistry or by a bulk electrolysis followed by spectral characterization. The thin-layer voltammograms were irreversible, and no intermediates were detected during the oxidation. The final spectra after the one-electron oxidation of (P)Ga(R) resembled the spectra of

(48) Nicholson, R. S.; Shain, I. *Anal. Chem.* **1964**, *36*, 707.

(P)GaCl; i.e., the spectra had a B(1,0) band and a Soret band shifted towards lower wavelengths. This is illustrated in Figure 9 for the case of (TPP)Ga(CH_3). Oxidation of all the tetraphenyl derivatives led to the same final species with a Soret peak at 423 nm and Q bands at 554 and 595 nm. Oxidation of the octaethyl derivatives also led to the same final species, which has a Soret band at 387 nm and Q bands at 534 and 572 nm. These spectra can reasonably be attributed to the corresponding (P)Ga(PF_6) complexes.

Comparison of (P)Ga(R) Reactivity with That of Other (P)M(R) Complexes. The reduction of organocobalt complexes leads to a cleavage of the cobalt-carbon bond.[49] In contrast, the addition of electrons to (P)In(R)[36] or (P)Ga(R) generates relatively stable singly and doubly reduced species. A stable anionic complex is also generated upon reduction of (P)Fe(C_6H_5),[50-52] but the reduction of iron porphyrin complexes with σ-bonded R groups such as C_6F_5 or C_6F_4H leads to rapid cleavage of the iron-carbon bond.[53] These differences in stability may result from differences in the site of electron transfer. The addition of an electron to the organocobalt complex and to (P)Fe(C_6F_5) involves reduction at the orbitals of the metal ion. This is not the case for (P)Ga(R) or (P)In(R), where anion radicals and dianions are formed. There is very little interaction of the σ-bonded ligand with the negatively charged conjugated π ring system, and this is reflected in the lack of substituent effects on the reduction potentials of (TPP)Ga(R) and (OEP)Ga(R).

It is also interesting to compare the chemical reactivity of singly oxidized $[(P)Ga(R)]^+$ with that of singly oxidized $[(P)In(R)]^+$, $[(P)Fe(R)]^+$, and $[(P)Co(R)]^+$. All three compounds are highly unstable, and after electrochemical generation from the corresponding $(P)M^{III}(R)$ derivative, each compound undergoes a rapid cleavage of metal-carbon bond.[15,36,51,52] They differ, however, in that both the iron and the cobalt derivatives undergo a metal to nitrogen migration resulting in the corresponding *N*-alkylporphyrin with an M(II) center. This migration does not occur during decomposition of $[(P)In(R)]^+$ or $[(P)Ga(R)]^+$, presumably due to the lack of an In(II) or Ga(II) oxidation state, which would be needed for the indium and gallium *N*-alkylporphyrin. In fact, to our knowledge, no indium or gallium *N*-alkylporphyrins have ever been synthesized.

Acknowledgment. The support of the National Science Foundation (Grant 8215507) is gratefully acknowledged. Discussions with Jean-Luc Cornillion regarding the (TPP)GaX and (OEP)GaX complexes are gratefully appreciated.

Registry No. (TPP)Ga($C(CH_3)_3$), 98943-15-8; (TPP)Ga($C(CH_3)_3$)$^+$, 98943-37-4; (TPP)Ga($C(CH_3)_3$)$^-$, 98943-23-8; (TPP)Ga(C_4H_9), 87607-78-1; (TPP)Ga(C_4H_9)$^+$, 98943-38-5; (TPP)Ga(C_4H_9)$^-$, 98943-24-9; (TPP)Ga(C_2H_5), 87607-77-0; (TPP)Ga(C_2H_5)$^+$, 98943-39-6; (TPP)Ga(C_2H_5)$^-$, 98943-25-0; (TPP)Ga(CH_3), 87607-76-9; (TPP)Ga(CH_3)$^+$, 98943-40-9; (TPP)Ga(CH_3)$^-$, 98943-26-1; (TPP)Ga($C_2H_2C_6H_5$), 98943-16-9; (TPP)Ga($C_2H_2C_6H_5$)$^+$, 98943-41-0; (TPP)Ga($C_2H_2C_6H_5$)$^-$, 98943-27-2; (TPP)Ga(C_6H_5), 87607-79-2; (TPP)Ga(C_6H_5)$^+$, 98943-42-1; (TPP)Ga(C_6H_5)$^-$, 98943-28-3; (TPP)Ga($C_2C_6H_5$), 98943-17-0; (TPP)Ga($C_2C_6H_5$)$^+$, 98943-43-2; (TPP)Ga($C_2C_6H_5$)$^-$, 98943-29-4; (TPP)GaCl, 78833-52-0; (TPP)GaCl$^+$, 98943-44-3; (TPP)GaCl$^-$, 98943-21-6; (TPP)Ga(*p*-MeC_6H_4), 87607-80-5; (OEP)Ga($C(CH_3)_3$), 98943-18-1; (OEP)Ga($C(CH_3)_3$)$^+$, 98943-45-4; (OEP)Ga($C(CH_3)_3$)$^-$, 98943-30-7; (OEP)Ga(C_4H_9), 87607-73-6; (OEP)Ga(C_4H_9)$^+$, 98943-46-5; (OEP)Ga(C_4H_9)$^-$, 98943-31-8; (OEP)Ga(C_2H_5), 87607-72-5; (OEP)Ga(C_2H_5)$^+$, 98943-47-6; (OEP)Ga(C_2H_5)$^-$, 98943-32-9; (OEP)Ga(CH_3), 87607-71-4; (OEP)Ga(CH_3)$^+$, 98943-48-7; (OEP)Ga(CH_3)$^-$, 98943-33-0; (OEP)Ga($C_2H_2C_6H_5$), 98943-19-2; (OEP)Ga($C_2H_2C_6H_5$)$^+$, 98943-49-8; (OEP)Ga($C_2H_2C_6H_5$)$^-$, 98943-34-1; (OEP)Ga(C_6H_5), 87607-74-7; (OEP)Ga(C_6H_5)$^+$, 98943-50-1; (OEP)Ga(C_6H_5)$^-$, 98943-35-2; (OEP)Ga($C_2C_6H_5$), 98943-20-5; (OEP)Ga($C_2C_6H_5$)$^+$, 98943-51-2; (OEP)Ga($C_2C_6H_5$)$^-$, 98943-36-3; (OEP)GaCl, 87607-70-3; (OEP)GaCl$^+$, 98943-52-3; (OEP)GaCl$^-$, 98943-22-7; (OEP)Ga(*p*-MeC_6H_4), 87607-75-8; TBA(PF_6), 3109-63-5.

(49) Lexa, D.; Saveant, J. M. *Acc. Chem. Res.* **1983**, *16*, 235.
(50) Lexa, D.; Saveant, J. M. *J. Am. Chem. Soc.* **1982**, *104*, 3503.
(51) Lancon, D.; Cocolios, P.; Guilard, R.; Kadish, K. M. *J. Am. Chem. Soc.* **1984**, *106*, 5724.
(52) Lancon, D.; Cocolios, P.; Guilard, R.; Kadish, K. M. *Organometallics*, **1984**, *3*, 1164.
(53) Guilard, R.; Boisselier-Cocolios, B.; Tabard, A.; Cocolios, P.; Simonet, B.; Kadish, K. M. *Inorg. Chem.* **1985**, *24*, 2509.

Contribution from the Department of Inorganic Chemistry, Indian Association for the Cultivation of Science, Calcutta 700032, India

Binding of a Nickel(IV) Complex to a Polyion-Modified Graphite Electrode: Electroprotic Equilibria

Rabindranath Mukherjee, Sreebrata Goswami, and Animesh Chakravorty*

Received December 17, 1984

The cationic $Ni^{IV}N_6$ complex, NiL^{2+}, of the hexadentate dioxime ligand (MeC(=NOH)C(Me)=$NCH_2CH_2NHCH_2$-)$_2$ (H_2L) has been incorporated by ion-exchange forces into poly(*p*-styrenesulfonate) (P-SS) films attached to a basal pyrolytic graphite (bpg) electrode surface over the pH range 1-9. Optimal binding is achieved in acidic solution (pH 3-5). The variable-pH cyclic voltammetry of the surface-bound complex has revealed that at pH <5 the single 2e-2H^+ couple $Ni^{IV}L^{2+}/Ni^{II}(H_2L)^{2+}$ (formal potential, $E^{\circ\prime}_{298}$, 0.72 ± 0.01 V) is operative. At alkaline pH, two 1e couples become observable: $Ni^{IV}L^{2+}/Ni^{III}L^+$ (0.42 ± 0.01 V) followed by $Ni^{III}L^+/Ni^{II}(HL)^+$ (0.66 ± 0.01 V; pH <8.5) or $Ni^{III}L^+/Ni^{II}L$ (0.17 ± 0.01 V; pH ≥8.5). This pattern of electroprotic equilibria is virtually the same as that observed for homogeneous aqueous solutions of NiL^{2+} at a bare bpg electrode. The cyclic voltammetric peak current of the surface-confined species (pH 4.05; 298 K) varies as the square root of scan rate over a wide range of surface coverage. The charge transport rate is thus slow, the diffusion coefficient being of the order of 10^{-9} cm^2/s. The equilibrium ratio of the concentration of NiL^{2+} in the polymer film to that in the loading solution is 30 ± 10 at 298 K and pH 4.05. The loss of incorporated NiL^{2+} from the loaded electrode into the buffer solution follows first-order kinetics with a rate constant of (3.5 ± 0.5) × 10^{-4} s^{-1} under the same conditions. In alkaline media such loss occurs at a higher rate on redox cycling presumably due to a diminution of ion-pair bond energy on reduction.

Introduction

The hexadentate amine-imine-oxime ligand[1] H_2L (**1**) and the conjugate oximato bases HL^- and L^{2-} display remarkable affinity for nickel and afford[2-4] pseudooctahedral NiN_6 species (**2**) spanning the oxidation states +2, +3 and +4. The structures of $[Ni^{IV}L](ClO_4)_2$ and $[Ni^{II}(H_2L)](ClO_4)_2$ are accurately known

(1) Ablov, A. V.; Belichuk, N. I.; Kaftanat, V. N. *Russ. J. Inorg. Chem. (Engl. Transl.)* **1972**, *17*, 392.
(2) Mohanty, J. G.; Chakravorty, A. *Indian J. Chem.* **1974**, *12*, 883. Mohanty, J. G.; Singh, R. P.; Chakravorty, A. *Inorg. Chem.* **1975**, *14*, 2178.
(3) Mohanty, J. G.; Chakravorty, A. *Inorg. Chim. Acta* **1976**, *18*, L33. Mohanty, J. G.; Chakravorty, A. *Inorg. Chem.* **1976**, *15*, 2912.

0020-1669/85/1324-4528$01.50/0